Supplementary Information

Nanoalloying Effect on Catalytic Activity of the Formate Oxidation Reaction over AgPd and AgCuPd Aerogels

Qiao Wang,[a,b] Fuyi Chen,[a,b,c*] Longfei Guo,[a,b] Tao Jin,[a,b] Huazhen Liu,[a,b] Xiaolu Wang,[a,b] Xiaofang Gong,[a,b] Yaxing Liu[a,c]

[a] State Key Laboratory of Solidification Processing, Northwestern Polytechnical University, Xi'an 710072, China

[b] School of Materials Science and Engineering, Northwestern Polytechnical University, Xi'an 710072, China

[c] School of Electronics and Information, Northwestern Polytechnical University, Xi'an 710072, China
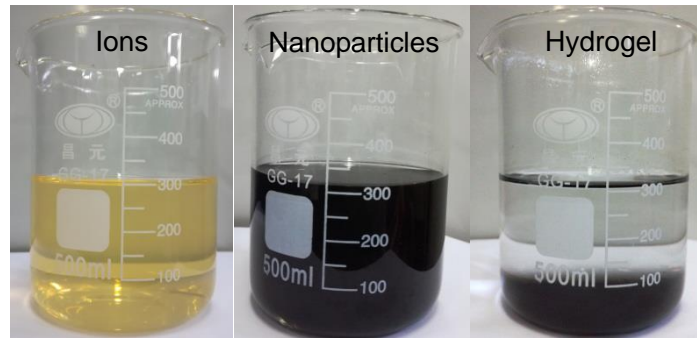
Figure S1 Digital pictures of $Ag_{50}Pd_{50}$ hydrogel formation at different stages.
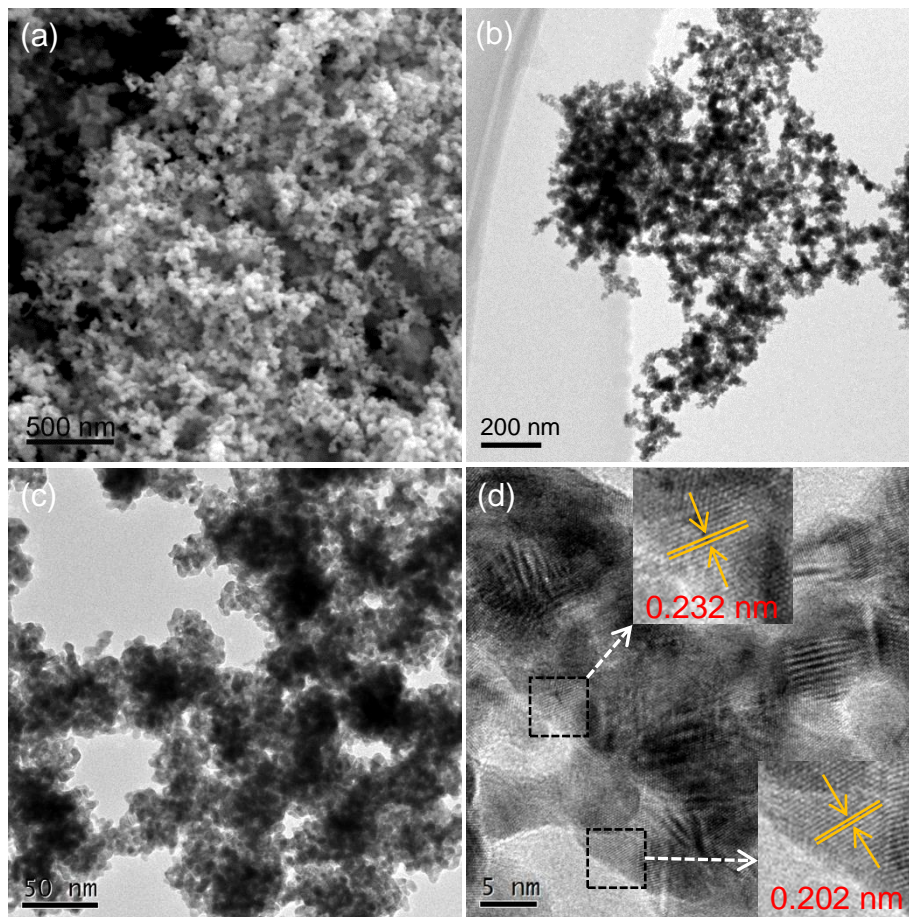

Figure S2 (a) SEM image. (b,c) Bright field TEM images. (d) HRTEM image of Pd aerogel. The inserts in (d) show the magnified HRTEM images.
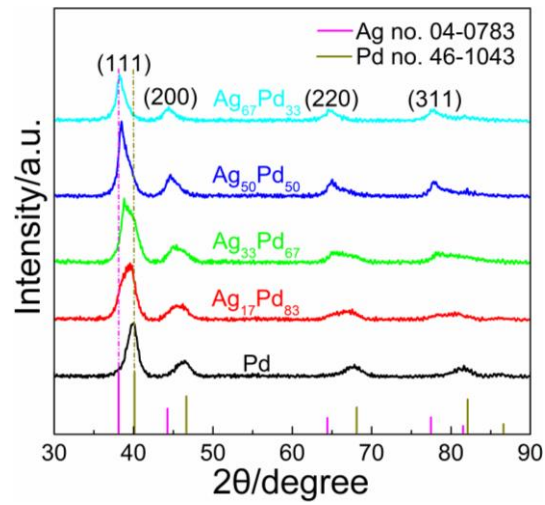
Figure S3 XRD patterns of Ag_xPd_{100-x} aerogels with various compositions, in comparison with standard peaks of Ag (no. 04-0783) and Pd (no. 46-1043).
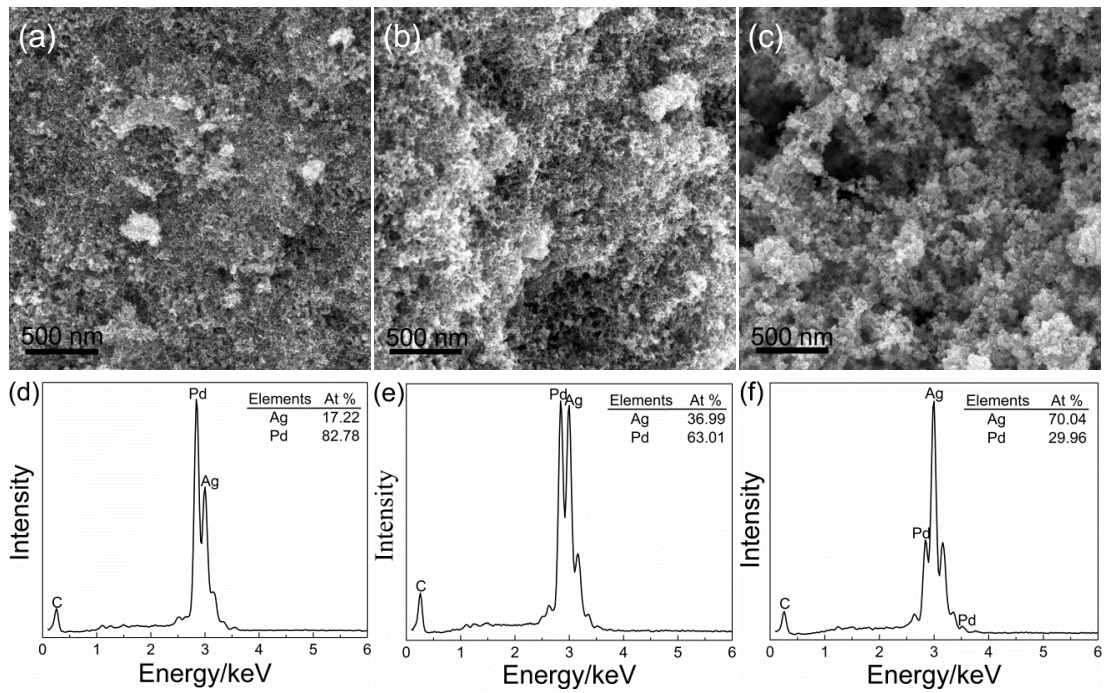

Figure S4 (a-c) SEM images of Ag_xPd_{100-x} aerogels with various compositions. (d-e) The corresponding SEM-EDS. (a,d) $Ag_{17}Pd_{83}$. (b,e) $Ag_{33}Pd_{67}$. (c,f) $Ag_{67}Pd_{33}$.
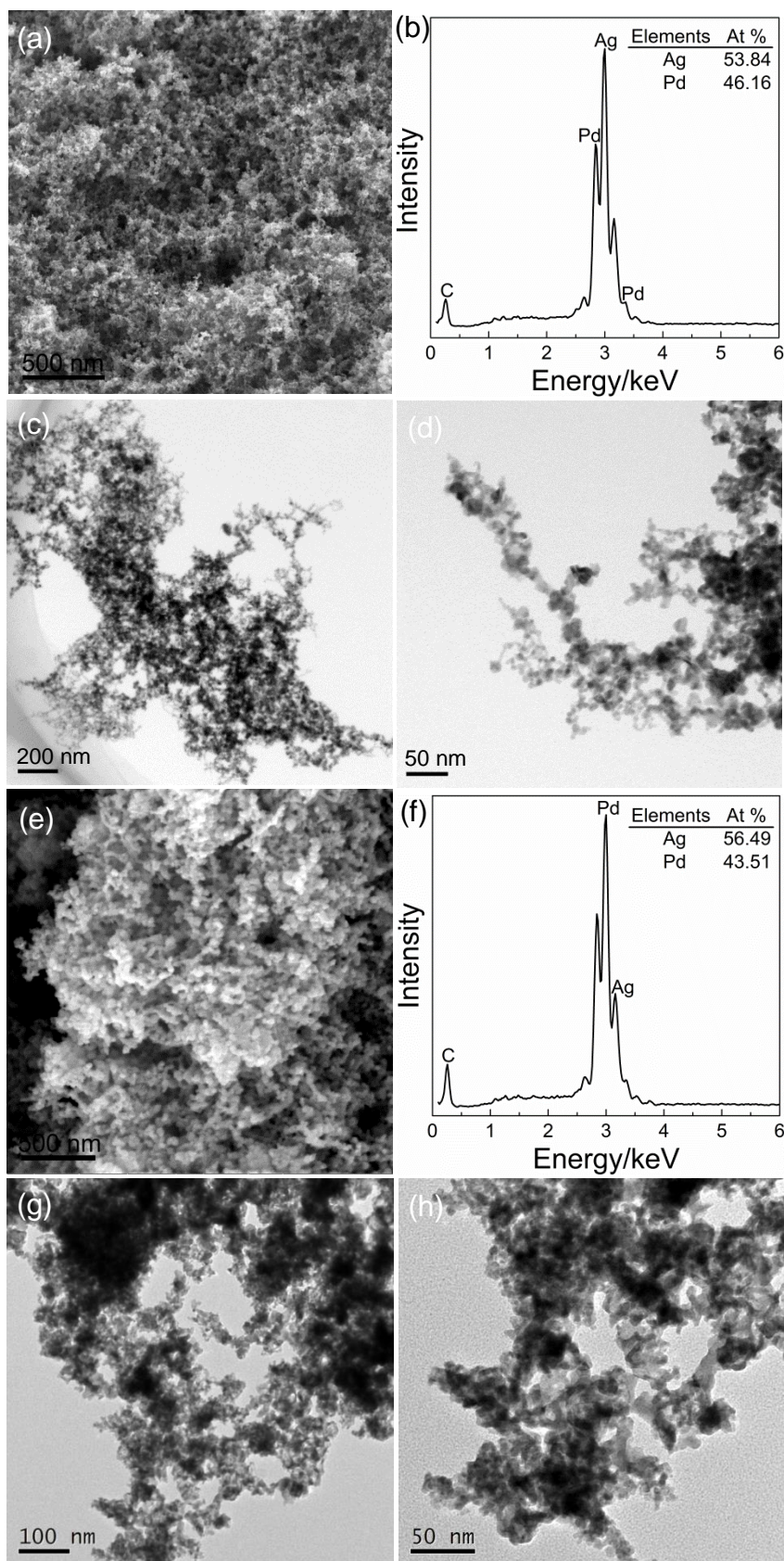
Figure S5 (a) SEM image. (b) SEM-EDS. (c,d) Bright field TEM images of AgPd aerogel when the concentration of metal precursors is 0.6 mM. (e) SEM image. (f) SEM-EDS. (g,h) Bright field TEM images of AgPd aerogel when the concentration of metal precursors is 5 mM.

The electrochemical active surface area (ECSA) of Pd-based catalysts can be calculated by quantification of the charges associated with the reduction of PdO, as shown in the following equation:

$$ECSA = Q / (c \times m)$$

Where, Q was the charge for PdO reduction on the surface, which can be obtained from integrating the shadow area as denoted in Figure S6. c was the charge required to reduce the PdO monolayer ($405 \ \mu C \ cm^{-2}$). m was the Pd mass on the working electrode (4.57 µg for $Ag_{50}Pd_{50}$). Thus, the ECSA value of $Ag_{50}Pd_{50}$ is $8.51 \ m^2 \ g^{-1}$.
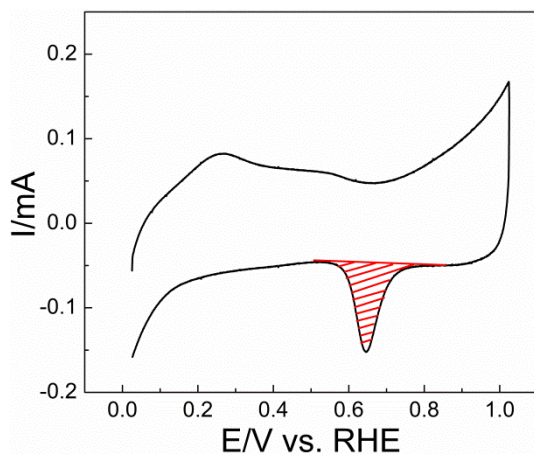

Figure S6 The CV curve of $Ag_{50}Pd_{50}$ recorded in N_2-saturated 1 M KOH solution at a scan rate of 50 mV s^{-1}.
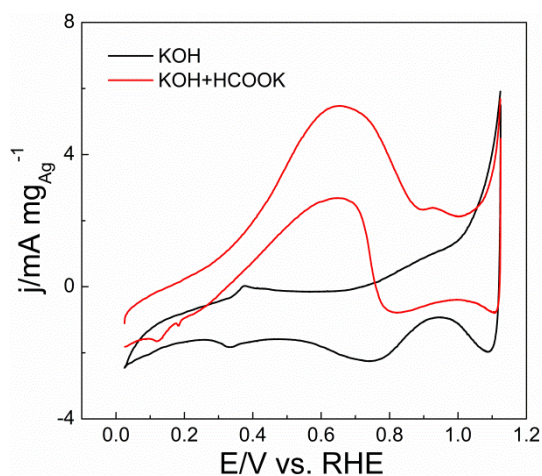

Figure S7 CV curves of pure Ag recorded in N_2-saturated 1 M KOH solution without and with 1 M HCOOK at a scan rate of 50 mV s^{-1}.
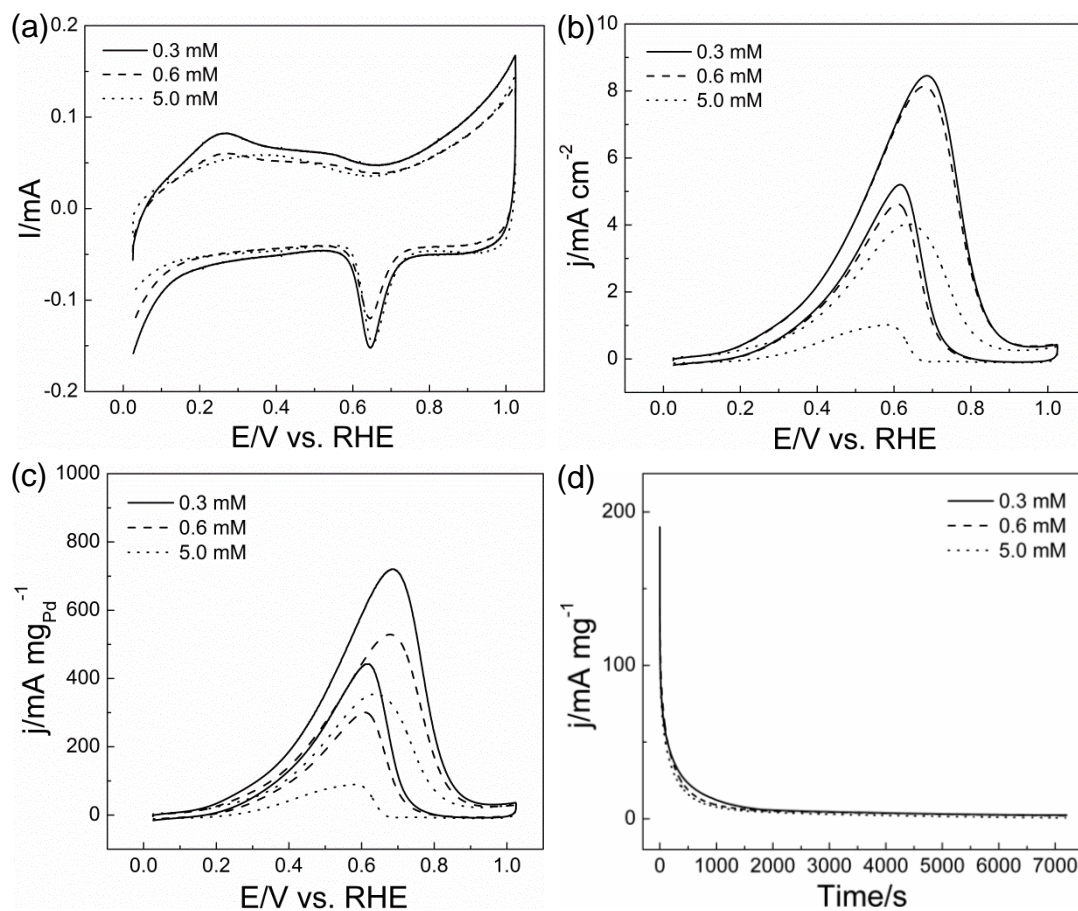
Figure S8 Electrocatalytic performance of AgPd aerogels when the concentrations of metal precursors are 0.3 mM, 0.6 mM, and 5 mM, respectively. (a) CV curves recorded in N_2-saturated 1 M KOH solution at a scan rate of 50 mV s^{-1}. (b,c) ECSA- and Mass- normalized CV curves for the FOR in 1 M KOH + 1 M HCOOK solution at a scan rate of 50 mV s^{-1}. (d) CA curves in 1 M KOH + 1 M HCOOK solution at 0.43V for 7200 s.
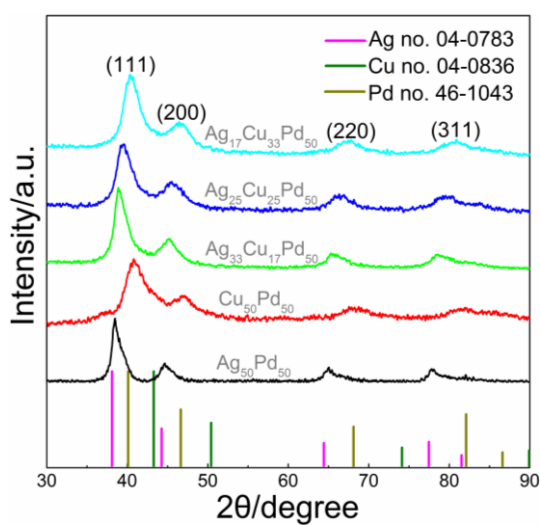

Figure S9 XRD patterns of Pd-based bimetallic and trimetallic catalysts, in comparison with standard peaks of Ag (no. 04-0783), Pd (no. 46-1043) and Cu (no. 04-0836).
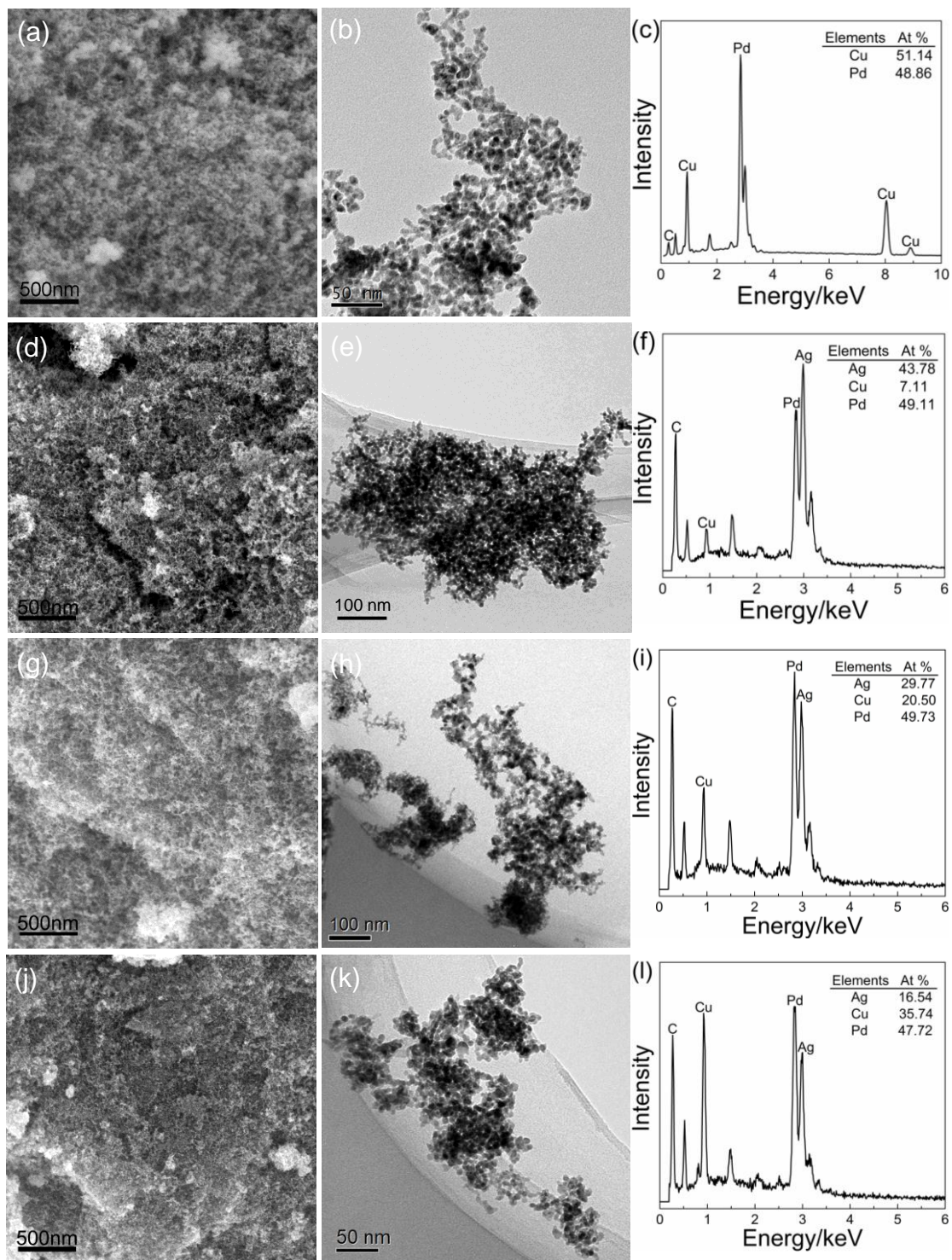
Figure S10 (a,d,g,h) SEM images. (b,e,h,k) Bright field TEM images. (c,f,i,l) SEM-EDS of the catalysts. (a-c) $Cu_{50}Pd_{50}$. (d-f) $Ag_{33}Cu_{17}Pd_{50}$. (g-i) $Ag_{25}Cu_{25}Pd_{50}$. (j-l) $Ag_{17}Cu_{33}Pd_{50}$.
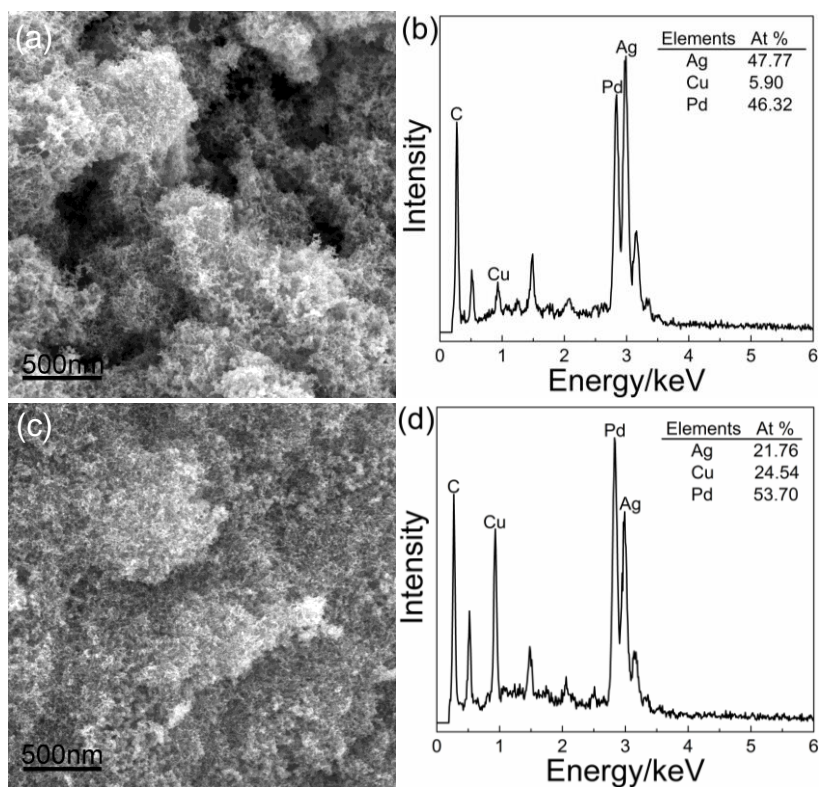
Figure S11 (a,b) SEM image and SEM-EDS of D-Ag$_{33}$Cu$_{17}$Pd$_{50}$ aerogel. (c,d) SEM image and SEM-EDS of D-Ag$_{17}$Cu$_{33}$Pd$_{50}$ aerogel.
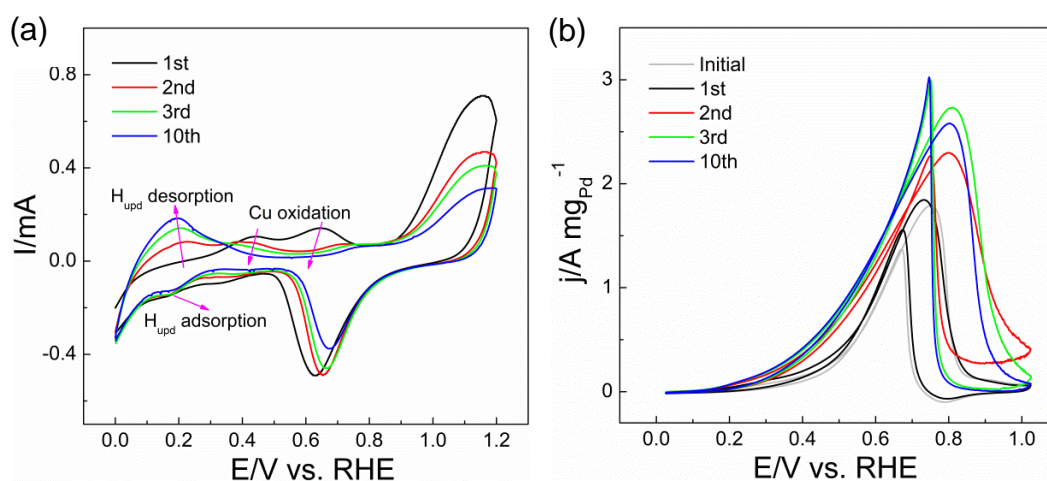
Figure S12 (a) CV curves recorded during dealloying at Ag$_{25}$Cu$_{25}$Pd$_{50}$-coated GC electrode at a scan rate of 50 mV s^{-1} in 0.1 M HClO$_4$ solution. (b) Mass- normalized CV curves recorded during dealloying in 1 M KOH + 1 M HCOOK solution at a scan rate of 50 mV s^{-1}.

Figure S13 (a-f) The CV curves of the Pd/C, $Ag_{50}Pd_{50}$, $Ag_{33}Cu_{17}Pd_{50}$, $Ag_{25}Cu_{25}Pd_{50}$, $Ag_{17}Cu_{33}Pd_{50}$, and D-$Ag_{25}Cu_{25}Pd_{50}$ catalysts before and after the CA test.

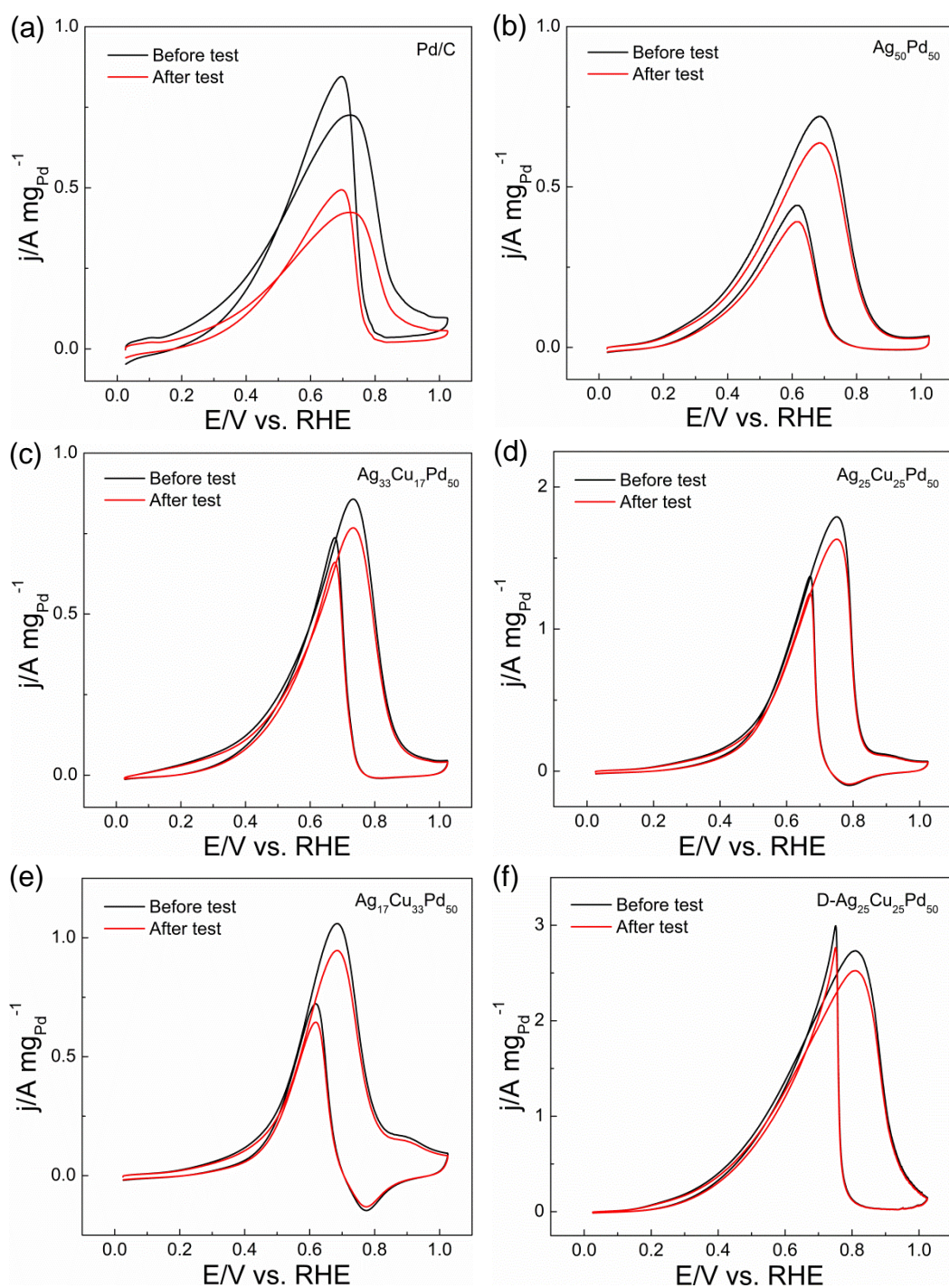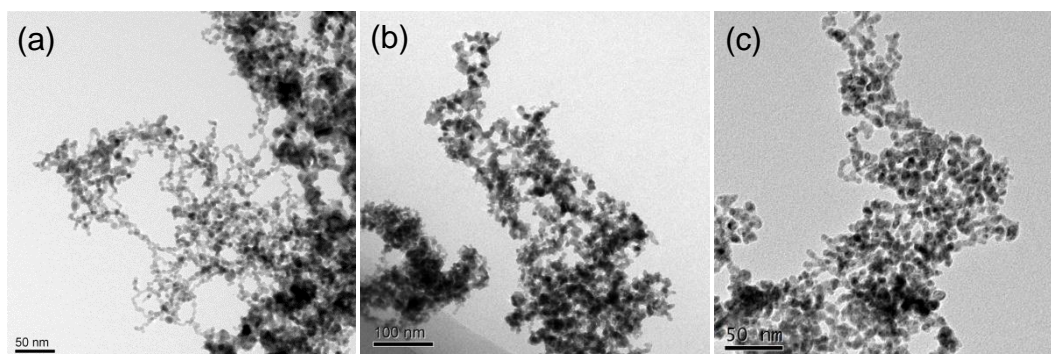Figure S14 TEM images of $Ag_{50}Pd_{50}$ (a), $Ag_{25}Cu_{25}Pd_{50}$ (b), and $D-Ag_{25}Cu_{25}Pd_{50}$ (c) after the stability test.
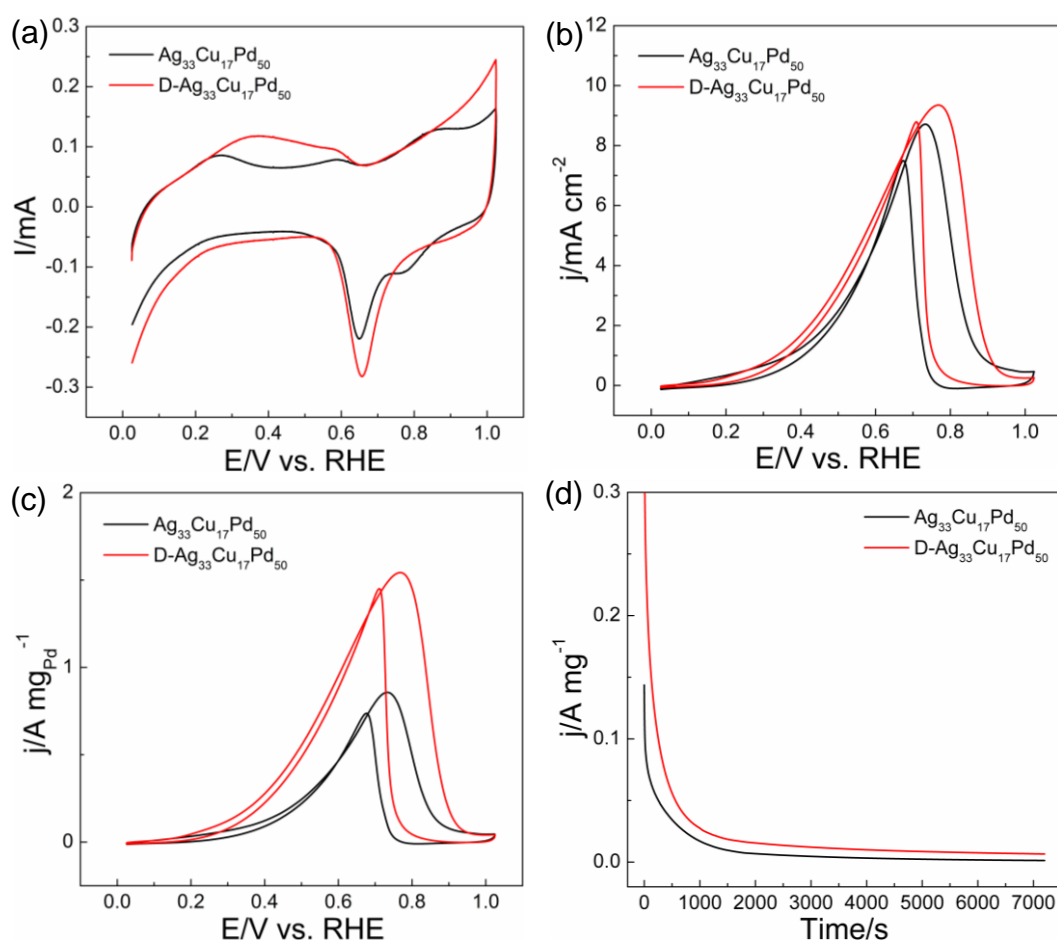
Figure S15 Electrocatalytic performance of $Ag_{33}Cu_{17}Pd_{50}$ before and after dealloying. (a) CV curves recorded in N_2-saturated 1 M KOH solution at a scan rate of 50 mV s^{-1}. (b,c) ECSA- and Mass- normalized CV curves for the FOR in 1 M KOH + 1 M HCOOK solution at a scan rate of 50 mV s^{-1}. (d) CA curves 1 M KOH + 1 M HCOOK solution at 0.43V for 7200 s.

Figure S16 Electrocatalytic performance of $Ag_{17}Cu_{33}Pd_{50}$ before and after dealloying. (a) CV curves recorded in N_2-saturated 1 M KOH solution at a scan rate of 50 mV s^{-1}. (b,c) ECSA- and Mass- normalized CV curves for the FOR in 1 M KOH + 1 M HCOOK solution at a scan rate of 50 mV s^{-1}. (d) CA curves 1 M KOH + 1 M HCOOK solution at 0.43V for 7200 s.
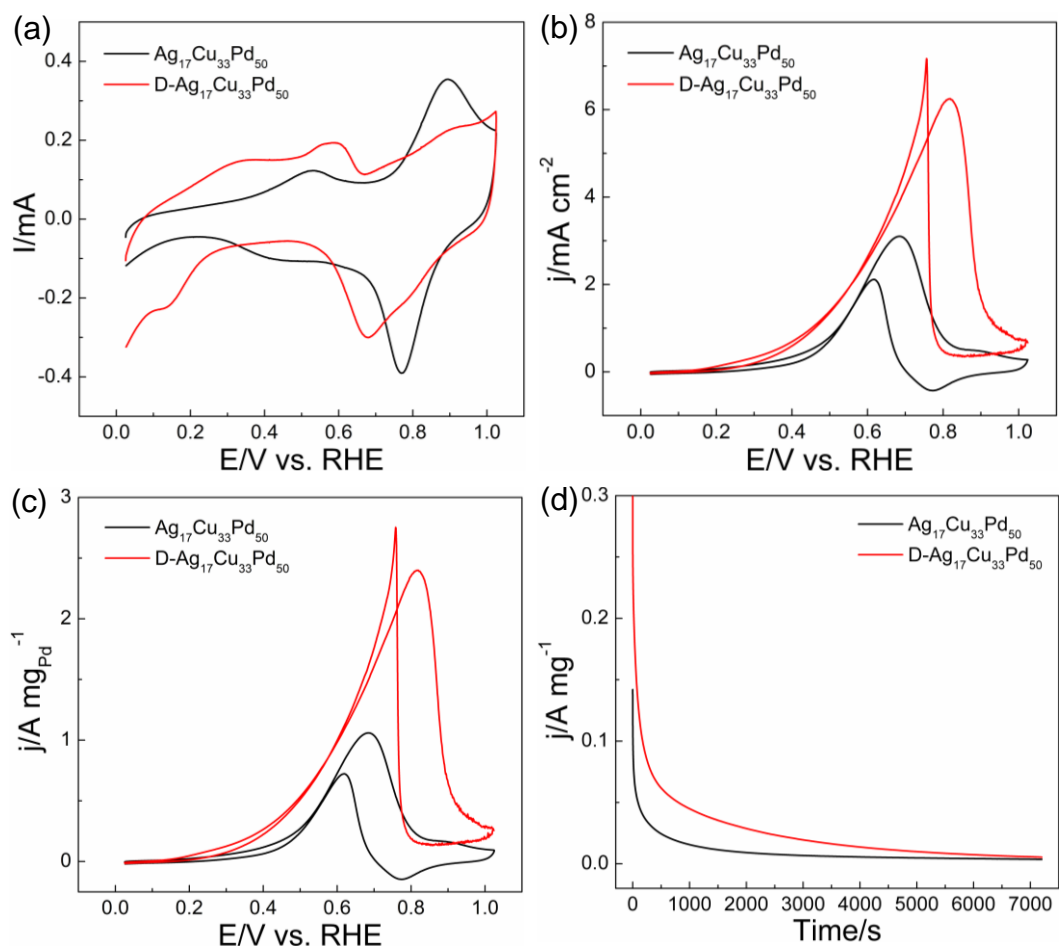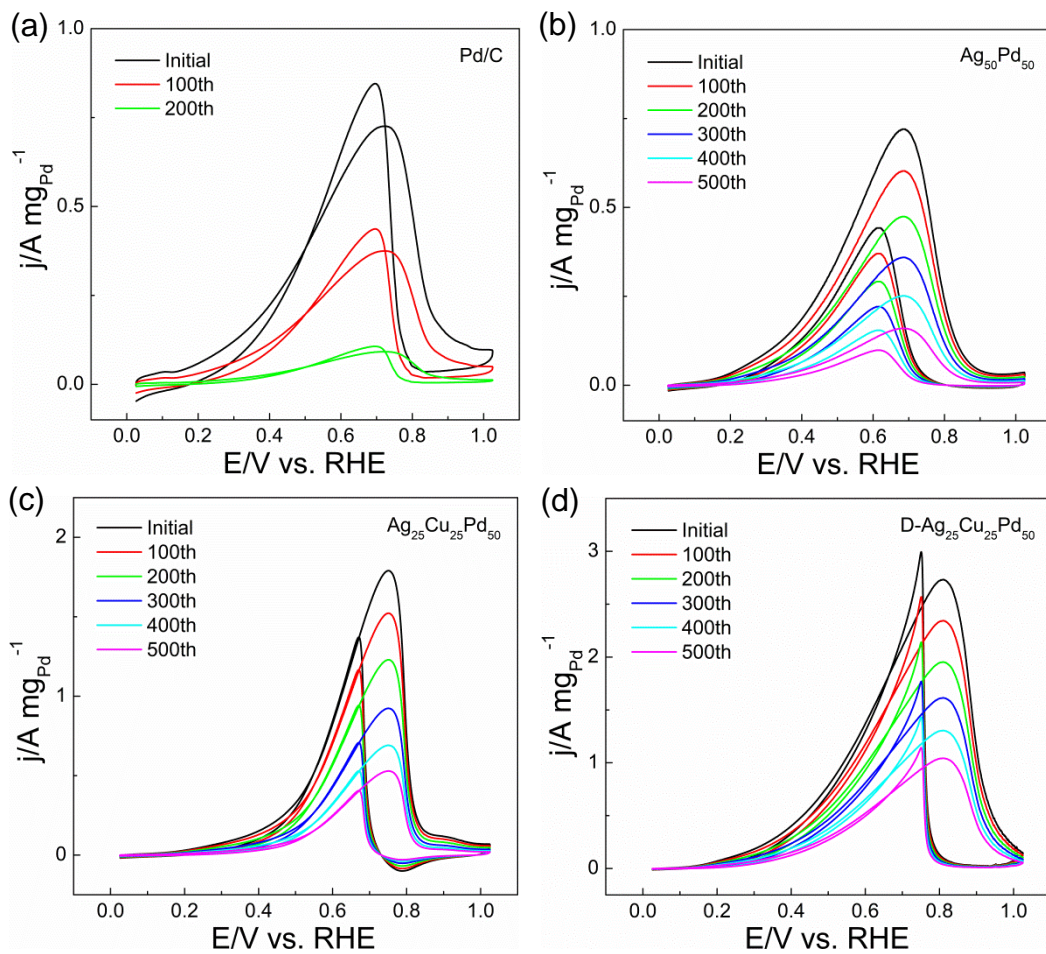
Figure S17 The cycling stability comparison of the catalysts towards the FOR. Multi-scanned CVs of (a) Pd/C (from 1st to the 200th cycle) and (b-d) $Ag_{50}Pd_{50}$, $Ag_{25}Cu_{25}Pd_{50}$, and D-$Ag_{25}Cu_{25}Pd_{50}$ catalysts (from 1st to the 500th cycle) in 1 M KOH + 1 M HCOOK solution.

Figure S18 The long-time stability of the D-$Ag_{25}Cu_{25}Pd_{50}$. The arrows show when the catalyst was reactivated and the electrolyte was exchanged.

Figure S19 (a) The XPS survey spectrum. (b) High-resolution Pd 3d XPS spectrum. (c) High-resolution Cu 2p XPS spectrum. (d) XPS Valence band spectrum and d-band center of $Cu_{50}Pd_{50}$ aerogel.

Table S1. A literature survey of the activity of Pd- and Pt- based FOR electrocatalysts in alkaline media.

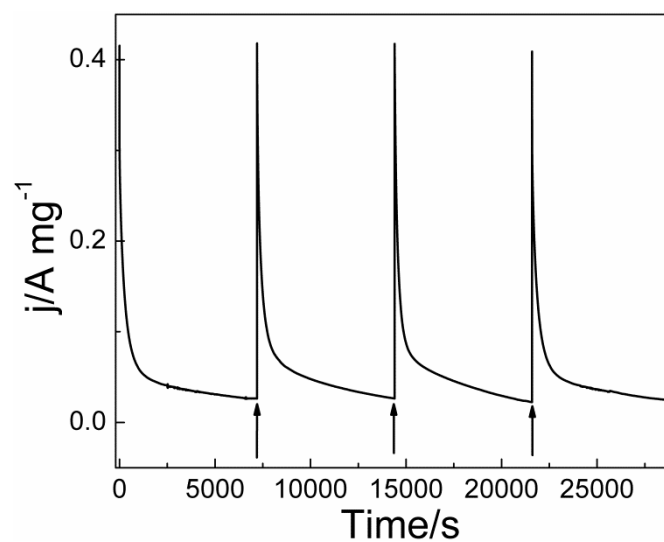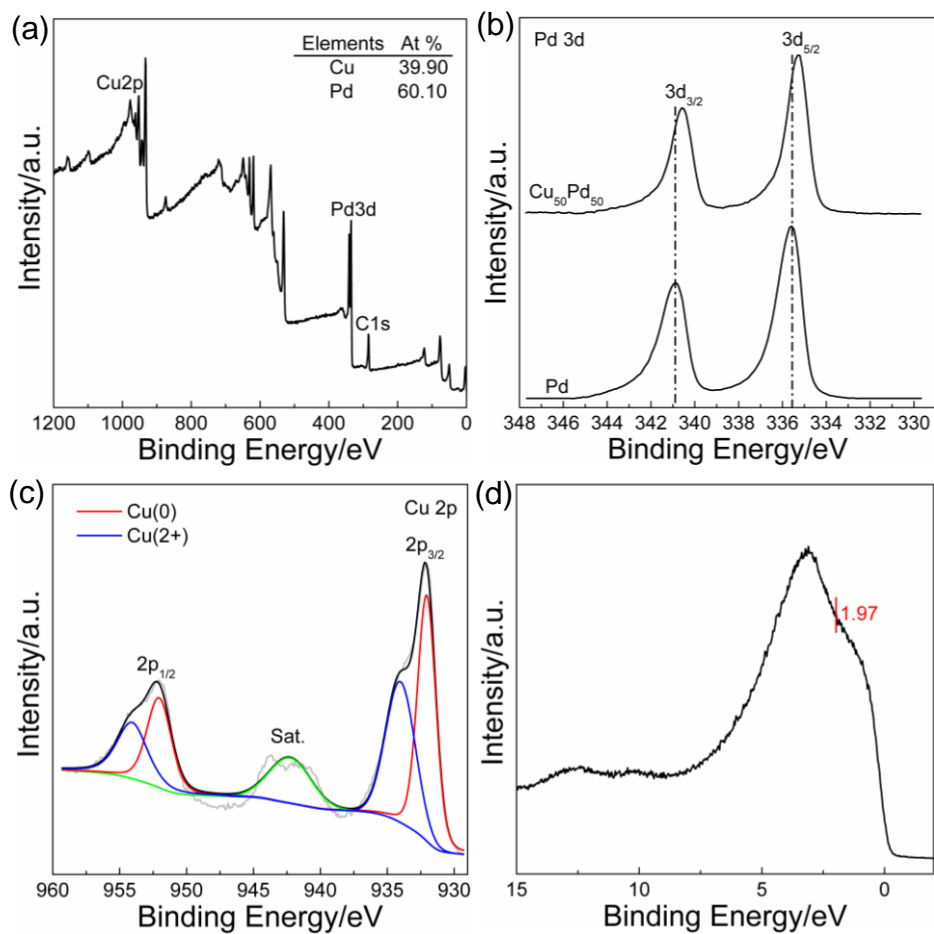| Electrocatalyst	Electrolyte	Scan rate $(mV\ s^{-1})$	ECSA $(m^2\ g^{-1})$	Specific activity $(mA\ cm^{-2})$	Mass activity $(mA\ mg^{-1})$	Reference
D-Ag$_{25}$Cu$_{25}$Pd$_{50}$ aergels	**1.0 M KOH + 1.0 M HCOOK**	**50**	**27.03**	**10.10**	**2735**	**This work**
Ag$_{25}$Cu$_{25}$Pd$_{50}$ aergels	**1.0 M KOH + 1.0 M HCOOK**	**50**	**15.01**	**9.86**	**1791**	**This work**
Ag$_{50}$Pd$_{50}$ aergels	**1.0 M KOH + 1.0 M HCOOK**	**50**	**8.51**	**8.45**	**719.91**	**This work**
Pd/C	2.0 M KOH + 2.0 M HCOOK	50	51.6	1.12	577.78	Appl. Energy 175 (2016) 479-487
PdH/C	1.0 M KOH + 0.1 M HCOOK	20	21.5	0.13	NA	Catal. Today 295 (2017) 26-31
Pd$_4$Ag/C	1.0 M NaOH + 0.1 M HCOONa	50	40.3	NA	40.0	Electrochim. Acta 225 (2017) 310-321
PdCu/C	1.0 M KOH + 1.0 M HCOOK	30	NA	3.46	NA	Electrochim. Acta 137 (2014) 654-660
Pd$_{2.3}$Co/C	1.0 M KOH + 1.0 M HCOOK	50	15	NA	2511	ACS Appl. Energy Mater.1 (2018) 4140-4149
PdAu/Ni foam	0.5 M NaOH + 0.1 M HCOONa	50	NA	0.75	NA	J. Power Sources 278 (2015) 569-573
CuPdAu/C	0.5 M KOH + 0.5 M HCOOK	50	45.1	NA	1150	Int. J. Hydrogen Energy 41(2016) 13190-13196
PtAu/C	2 M NaOH + 1 M HCOONa	10	NA	NA	0.011	Mater. Renew. Sustain. Energy 5 (2016) 1-8

Pt-Ag alloy nanoballoon nanoassemblies	1.0 M KOH + 1.0 M HCOOK	50	25.5	32.6	830	ACS Appl. Energy Mater. 1 (2018) 1252-1258

Table S2. The binding energies and surface composition in different catalysts by XPS analysis.

Electrocatalysts	Pd 3d$_{3/2}$ (eV)	Pd 3d$_{5/2}$ (eV)	Ag 3d$_{3/2}$ (eV)	Ag 3d$_{5/2}$ (eV)	surface composition	
					Pd (at%)	Ag (at%)
Pd	340.87	335.57	-	-	100	0
Ag$_{17}$Pd$_{83}$	341.07	335.77	374.07	368.07	72.56	27.44
Ag$_{33}$Pd$_{67}$	341.07	335.77	374.26	368.26	51.07	48.93
Ag$_{50}$Pd$_{50}$	341.07	335.77	374.27	368.27	38.28	61.72
Ag$_{67}$Pd$_{33}$	341.07	335.77	374.27	368.27	26.79	73.21
Ag	-	-	374.27	368.27	0	100